

Measuring and modeling postseismic motion associated with the 1999, M=7.1 Hector Mine earthquake

Teresa Baker\* working with Susan Owen\*\*

\*Massachusetts Institute of Technology; \*\*University of Southern California

Abstract

Following the October 16, 1999 M7.1 Hector Mine earthquake there has been a focused effort to collect postseismic surface deformation data in the region surrounding the ruptured fault. We calculated the velocity of the crust at over 40 locations around the rupture by determining precise relative positions using GPS. By measuring the postseismic deformation we can quantify the response of the crust and model the distribution of afterslip on the fault at depth. This is important to understanding the mechanics of the lower crust and the postseismic period of the earthquake cycle.

The postseismic deformation field follows the expected pattern of continued right-lateral displacement. The highest velocities occur 20-40 km from the surface rupture, indicating deep slip on the fault. Our models of the slip distribution at depth fit the overall pattern of surface deformation. The estimated distribution shows that postseismic deformation is consistent with deep afterslip occurring below the coseismic rupture depth.

The velocities subsided significantly over a nine month period. Taking this into account, we have modeled the distribution of slip over three time periods. It appears that the region of maximum slip moves northeast along the fault over time. Deeper slip

appears to follow below areas of shallow slip. Slip rates on the fault are much greater than deformation velocities at the surface.

## Introduction

The postseismic motion associated with the October 16, 1999 M7.1 Hector Mine earthquake is evidence of the continuing adjustment of the crust throughout the earthquake cycle. By observing the velocities at the surface in a large region surrounding the original rupture we can infer information about the rheology of the crust at depth. We can interpret the postseismic response of the crust at depth as brittle afterslip, viscoelastic relaxation or a combination of these. Using the surface motions we can model the distribution of slip on the fault at depth. With improved understanding of the distribution of slip we can begin to understand what strain conditions might cause another event on the fault, and when this might happen.

The Hector Mine earthquake was the largest earthquake to occur in California since the Mw7.3 Landers event in 1992. It ruptured parts of the Lavic Lake and Bullion faults, located 30 km to the east of the Landers surface trace in the eastern Mojave desert. Geologists mapped the rupture as extending 41 km with an average right-lateral, strike-slip offset of 300 cm (SRL, Vol. 71). The rupture trace is contained mostly within the Marine Corps Air-Ground Combat Center (MCAGCC) boundaries. The faults ruptured are part of the Eastern California Shear Zone (ECSZ), which is expected to take up 15% of the motion between the North American and Pacific plates (Sauber et al., 1986; Wesnousky, 1986).

We are measuring the motion of the surface using the Global Positioning System (GPS). GPS is a constellation of 27 satellites operated by the United States Department of Defense for navigational purposes. These satellites broadcast radio signals of two frequencies that contain information about transmission time and the position of the satellite. An antenna and receiver are set up on the ground to record the signal. The distance between the receiver and the satellite is determined by the transmission time times the speed of electromagnetic waves. The location of the receiver is constrained by the distance to a minimum of four satellites, the fourth being necessary to account for clock differences.

The original calculation of the distance is called the pseudorange because it does not account for many noise sources. Atmospheric interference, multipathing, and clock errors can affect the distance measurement. The interference of the ionosphere can be determined by the difference in time of arrival of the two frequency signals. The troposphere interference changes from hour to hour because conditions like humidity vary, but this effect is removed in postprocessing. Multipath is the satellite signal bouncing off nearby objects. The delay multipath causes is removed by a large ground plane on the antenna, blocking reflected signals, and by long recording periods. Clock error is caused by low quality clocks in the receivers while the satellites use more reliable atomic clocks. Many of the noise sources are removed by postprocessing in differential mode. By processing data using two concurrently running receivers and two satellites the errors in common fall out of the calculation. This gives high precision relative positioning, which allows us to see the centimeter scale postseismic motion associated with the Hector Mine

earthquake. These velocities can be observed in all three dimensions, which we refer to as North, East, and vertical.

The receivers can be set up in two different modes: campaign and continuous. Campaign data requires setting up an antenna, carefully centered and leveled over a benchmark for at least six hours per session. Small teams of scientists visit several sites during campaigns throughout the year. Survey-mode GPS allows data collection at many different sites, but each time the antenna is set up it will be at a different height, adding a possible error source. Continuous data collection uses a permanent set up of the same type of receiver and antenna. The antenna is attached to a tripod that is anchored to the ground and the anchor is cemented in place. Continuous data provides really good temporal coverage and human error in setup is not a factor. There are now global networks of continuous GPS setups coordinated by the International GPS Service. In Southern California there are many continuous sites monitored by Southern California Integrated GPS Network (SCIGN).

## Methodology

A continuing collaborative effort involving USC, UCSD, UCLA, the USGS, and MIT has been used to collect the GPS data for Hector Mine. New benchmarks have been installed to increase coverage of the area, including continuous sites on the Marine base. A team of researchers collected survey-mode GPS data at 39 geodetic markers in the first two weeks following the earthquake. Observing sites on the marine base requires coordination with the Windows of Opportunity at MCAGCC. Fortunately there were already

several permanent sites set up west of the fault as part of the SCIGN array. We have used sites that are part of the SCIGN network to increase coverage.

We used GIPSY OASIS II to postprocess the data and determine locations for all of the sites relative to a station located in Blythe, a significant distance from the rupture. GIPSY OASIS II uses orbit ephemeris calculations and satellite clock corrections from Jet Propulsion Laboratory and incorporates physical Earth models, such as the troposphere at the time of the observation. The program outputs station positions for each day, and a covariance matrix. These positions are given in International Terrestrial Reference Frame 1997. We processed the data in two groups, one including far field stations and the other involving the most pertinent local stations. We included data for three stations in central United States in the far field group so a tie can be made to stable North America.

Using Matlab we made an estimate for the velocity of each station. Looking at the time series for each station we removed anomalous data caused by an antenna slipping, problems with the receivers, or insufficient data. In the time series there is a clear decay in velocity for many of the stations. We also looked at the velocities as a map showing a vector for each station. On this map we can observe the right lateral trend of motion, which follows the coseismic motion. It is also possible to look for the distance from the fault showing the greatest surface velocity and infer significant slip occurring similarly at that depth below the rupture.

We modeled the distribution of slip on the fault at depth based on the surface velocities. The method involves inverting the following equation of matrices:

$$\mathbf{d} = \mathbf{G} \mathbf{m}$$

The  $\mathbf{d}$  matrix contains the velocity of each station, relative to the reference station. The  $\mathbf{G}$  matrix contains the fault parameters, including depth, width, length, and location of the fault. Matrix  $\mathbf{m}$  contains the model parameters. We modeled the fault by extending down 40 km below the mapped surface rupture. This plane is divided into 2 km square finite elements. The model parameters are the slip on each element. We used Matlab to include second derivative smoothing to improve the model coherence.

The best-fit model is found by inverting the  $\mathbf{G}$  matrix and solving for  $\mathbf{m}$ . The values in  $\mathbf{m}$  can be affected by changing the parameters of the fault geometry, including the length of the fault and the depth it is extended to. The slip distribution is also affected by requiring the slip to smooth to zero at various edges of the fault plane. We extended the fault by 20 km on either side of the rupture based on aftershock seismicity. We looked for parameters for which the sensitivity of the solution to smoothing to zero at the edges and small changes in the length and depth of the fault is least. After testing the effect of different fault parameters and smoothing requirements, we chose the best model based on its fit to the data and plausibility. Models fitting the data perfectly have unreasonable and incongruous slip rates. Also several models showed negative (left-lateral) slip on the fault at depth, but we considered Hector Mine earthquake and its postseismic response to involve solely right-lateral motion.

## Discussion

Looking at the time series for several stations there is a significant decay in the surface velocities, occurring mainly in the first 40 days following the earthquake. The slower deformation occurring after the first 40 days may not subside to interseismic

velocities for three years following the temblor, based on studies of the motion following Landers (Savage).

The velocity maps (figures 1a,2a,and 3a) show continued right lateral motion along the fault. The trend of the vectors makes an x pattern centered on the fault. The change in velocity directions at the ends of the fault is an expected edge effect. The largest velocities appear 20-40 km to either side of the fault. This indicates deep afterslip on the fault. This surface motion is located in near proximity to the Landers fault on the western side, but is also seen on the eastern side of the Bullion and Lavic Lake faults. Motion associated with Landers is expected to have subsided to near interseismic velocities. The stations in the southwest corner of our network are affected by interseismic deformation along the San Andreas. To remove this effect we modeled the surface deformation caused by the San Andreas using a locking depth of 15 km and slip rates of 12 - 30 mm/yr.

We modeled the distribution of slip on the Hector Mine fault over three different time periods: October 17 - November 30, October 17 - January 15, and November 30 - June 06. The first 40 days following the earthquake was chosen as the first time period based on the decay in surface velocities seen in the time series. The second time period was chosen to accomodate differences in temporal coverage between survey-mode and continuous data. Several of the sites were last visited in January at the time of the processing. The third time period models the slip distribution through June, but excludes the first 40 days of rapid decay.

Figures 1b, 2b, and 3b show our best-fit model for each time period. The slip rates at depth are at least a magnitude larger than the surface deformation velocities. Over

the first time period these rates reach 1.2 m/yr, whereas in the period excluding the first period, rates are approximately half this. For all three periods the slip is focussed at 40 km depth. Models using shallower depths had poorer fits to the data.

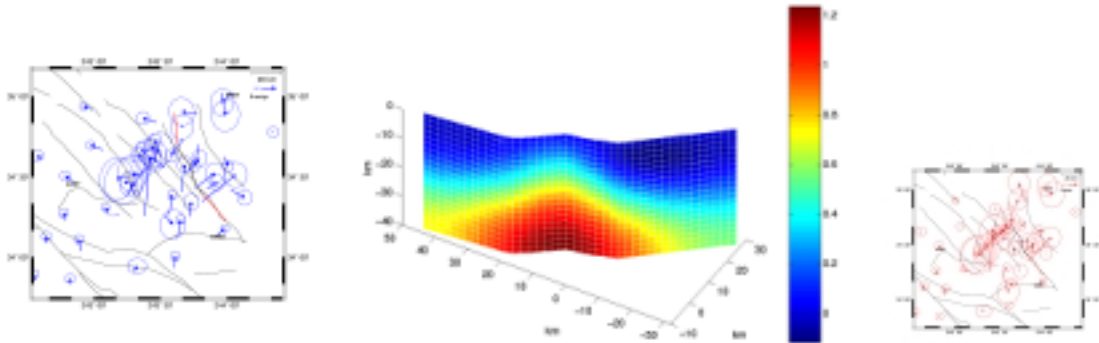


Figure 1(a-c) Velocities, slip distribution model, and residuals for October — November. Black lines represent faults. Ellipses are for 95% confidence.

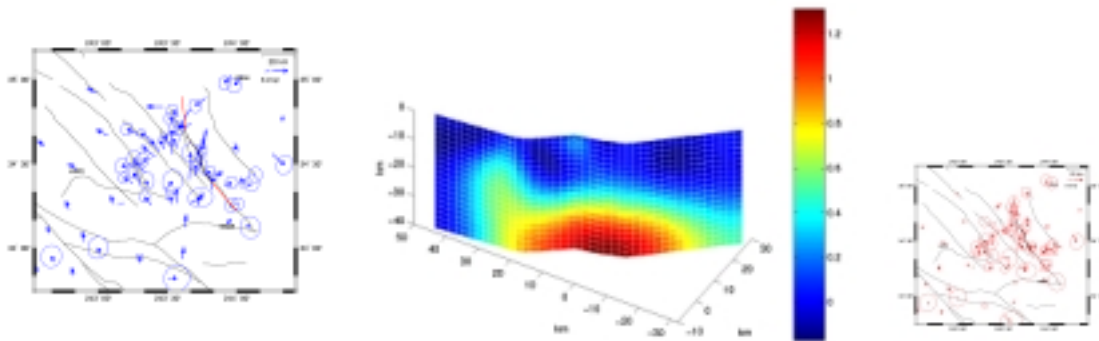


Figure 2(a-c) Velocities, slip distribution model, and residuals for October- January.

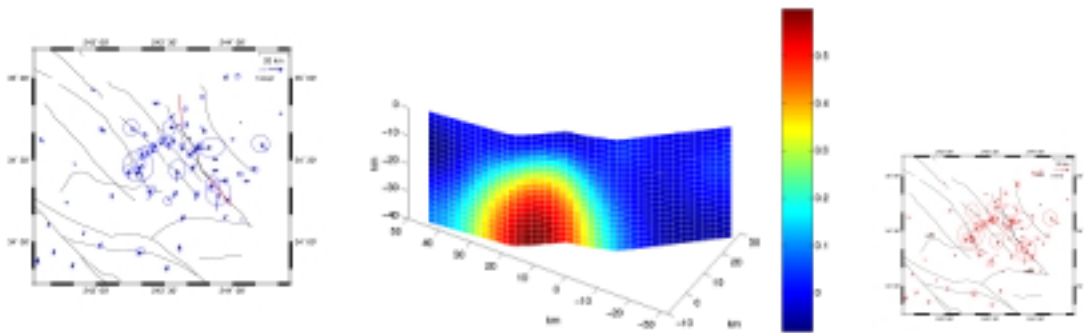


Figure 3(a-c) Velocities, slip distribution model, and residuals for November — June.

The slip distribution for the first time period is highly symmetrical, which is similar to the motion along the fault during the temblor. The focus of slip occurs roughly below the epicenter. There is little or no slip on the upper 8 km of the fault, which corroborates the idea that slip in the upper crust occurred coseismically and now the deep crust is catching up. This model is not particularly sensitive to constraining the slip at the edges of the fault plane to be zero.

In figure 2b the slip distribution takes on shape. The slip focus is further to the southwest along the fault. Shallower slip occurs on the northeastern part of the fault. This model uses the average velocities for the three month period following the earthquake, which is why areas with slip in the first model can appear to have zero slip in figure 2b. Figure 3b shows the model for the third time period. The slip focus has moved northeast along the fault, and is now located below the area of shallow slip in figure 2b.. There is no slip occurring on the southwest part of the fault.

The models show slip distributions that fit the deformation we see at the surface. Model velocity vectors are created working backward from the model. The model veloc-

ity vectors can be plotted on top of the observed velocities, and vectors with tips lying inside the 95% confidence level error ellipse are considered an acceptable fit to the data. Figures 1c, 2c, and 3c show the error residuals for each model. The vector represents the model velocity minus the observed velocity. The ellipses are the same as those in the velocity maps in 1a, 2a, and 3a. Vectors contained completely within the ellipse represent data fit to the 95% confidence level. While the existence of a rigid fault plane at 40 km depth is questionable, we are able to fit the observed surface deformation using this model.

#### Conclusion

Postseismic surface deformation associated with Hector Mine continues in right-lateral orientation, with velocities greater than the expected interseismic velocities. The surface velocities decay most rapidly in the first 40 days following the earthquake. Slip distribution models show rates of 1.2 m/yr at 40 km depth for the first 40 days. In subsequent deformation the distribution becomes more focused and moves northeast along the fault, filling in areas of shallower slip. We are able to fit the data fairly well using slip distributed on the plane at depth, however models of viscoelastic relaxation could improve this fit. Further work could include adding a second fault plane based on aftershock seismicity. Comparisons and combinations of GPS and InSAR data can also be made. Further campaigns are planned to extend the time series until the postseismic motion subsides to the estimated interseismic rate.

## Acknowledgements

I would like to thank Southern California Earthquake Center for making this internship possible. I also greatly appreciate the guidance and mentorship of Susan Owen..

## References

Gregorius, Thierry, GIPSY-OASIS II How it works..., University of Newcastle upon Tyne, October, 1996.

Savage, J.C. and J.L. Svarc, Postseismic deformation associated with the 1992 M=7.3 Landers earthquake, Southern California, Journal of Geophysical Research, vol. 102, No. B4, Pages 7565-7577, April 10, 1997.

<http://pasadena.wr.usgs.gov/hector>

Pollitz, Fred, and Roland Burgmann, Joint estimation of the afterslip rate and postseismic relaxation following the 1989 Loma Prieta earthquake, Journal of Geophysical Research, Vol. 103, No. B11, Pages 26, 975-26, 992, November 10, 1998.

Sauber, J., W. Thatcher, S.C. Solomon, Geodetic measurement of deformation in the central Mojave desert, California, J. Geophys. Res., 91, 2683-2693, 1986.

US Geological Survey, Southern California Earthquake Center, and California Division of Mines and Geology, Preliminary Report on the 16 October M7.1 Hector Mine, California Earthquake, Seismological Research Letter, Vol. 71, Number 1, 11-23.

Wesnousky, S., Earthquakes, Quaternary faults, and seismic hazard in California, J. Geophys. Res., 91, 2587-2631. ber 1, 11-23, 1986.